

Effect of Various Divalent Ions on the Calcium Current of Adrenal Medullary Chromaffin Cells in the Rat

Jun Kim, Chae Hun Leem and Sang Jeong Kim

Department of Physiology & Biophysics, Seoul National University College of Medicine, Seoul 110-799, Korea

= ABSTRACT =

It is well known that chromaffin cells of adrenal medulla secrete catecholamine in response to sympathetic nerve activation and the influx of Ca^{2+} through the voltage dependent Ca^{2+} channels (VDCC) in the cell membrane do a major role in this secretory process. In this study, we explored the effect of divalent cations on VDCC of rat chromaffin cells.

Rat (Sprague - Dawley rat, 150 - 250 gm) chromaffin cells were isolated and cultured. Standard giga-seal, whole-cell recording techniques were employed to study Ca^{2+} current with external and internal solutions that could effectively isolate VDCC currents (NMG in external and TEA and Cs^{2+} in internal solution).

The voltage dependence and the inactivation time course of VDCC in our cells were identical to those of bovine chromaffin cells. A persistent inward current was first activated by depolarizing step pulse from the holding potential (H.P.) of -80 mV to -40 mV, increased to maximum amplitude at around $+10$ mV, and became smaller with progressively higher depolarizing pulses to reverse at around $+60$ mV. The inactivation time constant (τ), fitted from the long duration test potential (2 sec) was 1295.2 ± 126.8 msec ($n=20$, 1 day of culture, mean \pm S.E.M.) and the kinetic parameters were not altered along the culture duration. Nicardipine ($10 \mu\text{M}$) blocked the current almost completely. Among treated divalent cations such as Cd^{2+} , Co^{2+} , Ni^{2+} , Zn^{2+} and Mn^{2+} , Cd^{2+} was the most potent blocker on VDCC. When the depolarizing step pulse from -80 mV to 10 mV was applied, the equilibrium dissociation constant (K_d) of Cd^{2+} was $39 \mu\text{M}$, K_d of Co^{2+} was $100 \mu\text{M}$ and K_d of Ni^{2+} was $780 \mu\text{M}$.

The principal findings of this study are as follows. First, the majority of Ca^{2+} channels in rat chromaffin cells are well classified to L-type Ca^{2+} channel in the view of kinetics and pharmacology. Second, all divalent cations tested could block the Ca^{2+} current and the most potent blocker among the tested was Cd^{2+} .

Key Words: Rat chromaffin cell, calcium current, L-type calcium channel, divalent cation

INTRODUCTION

It is well known that the chromaffin cell of adrenal medulla secretes catecholamine in response to sympathetic nerve activation and that Ca^{2+} does a major role in this secretory pro-

cess (Douglas, 1968; Augustine & Neher, 1992). The main source of Ca^{2+} is considered to originate from the influx of Ca^{2+} through the Ca^{2+} channels (Douglas, 1975; Wakade et al., 1986), in spite of the view that Ca^{2+} originates from internal reservoir like the endoplasmic reticulum after muscarinic receptor activation.

Recently, it has been reported that excitable membrane of neuronal tissue possesses three types of Ca^{2+} channels: L-, N-, T-type channels (Nowycky et al, 1985; Fox et al, 1987). According to electrophysiological study on Ca^{2+} channel, the bovine chromaffin cell contains L-type

This study was supported by a 1991 RESEARCH GRANT from the MINISTRY OF EDUCATION and the 1992 Research Promoting Fund of Seoul National University College of Medicine

Ca²⁺ channel (Cena et al., 1989; Tsien et al., 1988). It is reported, by the radioligand binding study, that the bovine chromaffin cell contains two types of Ca²⁺ channels (Ballesta et al., 1989). Some of recent electrophysiological studies suggest that two types of Ca²⁺ channels exist in chromaffin cell (Rosario et al., 1989; Artalejo et al., 1990; 1991a). There are many arguments on the characteristics of L-type Ca²⁺ channel of chromaffin cell. For example, Tsien et al. (1988) reported that L-type channels of chick sensory neuron was blocked by Cd²⁺ and Ni²⁺ but the amount of catecholamine from the adrenal gland perfused with Cd²⁺ or Ni²⁺ containing solution was not decreased but the secretion was blocked by the Zn²⁺ and Mn²⁺ (Shukla & Wakade, 1991). In subsequent report, the type of Ca²⁺ channel other than L- and N-type Ca²⁺ channel was also suggested in bovine chromaffin cell (Artalejo, 1991b).

In this study the cultured chromaffin cells were isolated from the rat adrenal gland and the effects of divalent cations and organic antagonists on Ca²⁺ current of these cells were explored using whole cell voltage clamp method. From the results of this study it is possible to explore the consistency of Ca²⁺ channel classification, suggested by Tsien et al. (1988), on rat chromaffin cells and to compare the blocking effects of various divalent cations on Ca²⁺ channel currents.

METHODS

Cell culture

Rat chromaffin cells were obtained by the method modified from Akaike et al. (1990) using Sprague-Dawley rat (150 - 250 gm). Adrenal glands were isolated from the spinalized rat with aseptic procedure and transferred to the Ca²⁺-free buffer of pH 7.4 to dissect adrenal medulla surgically under dissecting microscope. The isolated tissue of medulla was minced to 1 mm³ and the supernatant was removed after centrifugation (1000 RPM, arm length 40cm, 7 min). The remnant tissue was dissociated into single cells by a 30 min incubation (35°C) in a

Ca²⁺ free buffer containing 0.2 % collagenase (Sigma, type I), followed by gentle trituration in the buffer with Ca²⁺ (2mM) and bovine serum albumin(0.5 %). The isolated cells were purified with 20 % percoll density gradient (2000 RPM, 12 min) and the purified cells were plated on poly-L-lysine coated coverslips and maintained in Dulbecco's modified Eagle's medium with the following supplements: 10 % fetal bovine serum, 50 u/ml penicillin, 50 gm/ml streptomycin, 2mM glutamine, 1mM pyruvate, 0.5 % glucose. The cells were used after 1 day's rest until the 7th day of culture.

Electrical signal recording

Standard whole-cell recording techniques (Hamill et al, 1981) were used to study Ca²⁺ channel of the rat chromaffin cell. A List EPC-7 patch-clamp amplifier were used and microelectrodes were prepared with Kimax-51 borosilicate capillary tubes (Kimble, USA). The tips of electrodes were coated with sylgard to reduce capacitive current and remnant capacitive transients were routinely cancelled using the EPC-7 amplifier's cancellation circuitry. Pulse generation, data acquisition, subtraction of linear leak and capacitive currents, and data analysis were performed using PCLAMP software (Axon Instruments, USA). For patch clamp experiments, rat chromaffin cells on the culture coverslips were transferred to a recording dish (modified from 35mm-culture dish) filled with 3 ml bath solution containing (in mM): 143 N-methyl D-glucamine (NMG), 10 CaCl₂, 0.5 MgCl₂, 5.4 KCl and 5 N-2-hydroxyethylpiperazine-N''-2-ethanesulfonic acid (HEPES), adjusted to pH 7.2. Electrode-filling solution contained (in mM): 120 CsCl, 2 MgCl₂, 11 EGTA, 1 CaCl₂, 10 HEPES, with the pH adjusted to 7.2 with CsOH. The electrodes of which the resistance was between 2MΩ and 3MΩ were used. After a gigaseal was formed, the patch was ruptured by gentle suction to make a whole cell clamp configuration. To give the enough time for diffusion of the electrode solution into cell, current recordings were started after 1 min from the rupture. All the experiments were performed

at room temperature (20–25°C) and within 1 hour after the cells were transferred from the CO₂ incubator.

Experimental protocol

Control currents were recorded from the first coverslip and each experimental condition was given to another coverslip. We recorded at least 3 cells from a coverslip and the effects were evaluated with statistical method. 100 times concentrated stock solutions of Cd²⁺, Co²⁺, Ni²⁺, Zn²⁺, Mn²⁺ and dihydropyridine were used. Exposure to light was minimized during dihydropyridine study. To evaluate the voltage dependence of Ca²⁺ channel, depolarizing step pulses of 150 ms duration were applied and long test depolarizations of 2 sec were applied for the evaluation of inactivation time constant (τ).

Statistics

The statistical significance of differences between the values was determined using the non-paired Student's *t*-test and the analysis of variance (ANOVA) method. All the statistical values were expressed in mean \pm S.E.M. (standard error).

RESULTS

Kinetics of Ca²⁺ current in rat chromaffin cell

For recording Ca²⁺ current, Na⁺ current was eliminated by total replacement of Na⁺ with N-methyl-D-glucamine (NMG) and K⁺ current was minimized by TEA and Cs⁺ in pipette solution. Holding potential (H.P.) was -80 mV. Figure 1A shows Ca²⁺ current traces evoked by depolarizations to various test potentials (V_t ; 150 ms duration). In Figure 1B its current-voltage (*I*-*V*) relationship was shown. The current amplitude in *I*-*V* curve was obtained from the difference between averaged value of holding current and averaged steady state current amplitude (area of bar in Fig. 1A). Apparent inward current appears first at about -40 mV and grows to maximum amplitude at

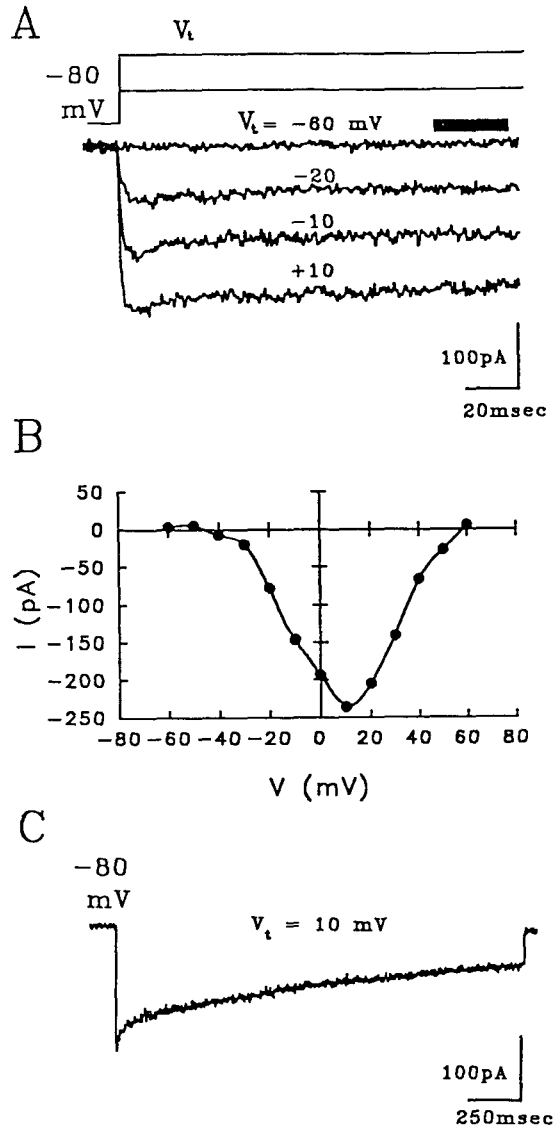


Fig. 1. Kinetics of Ca current in rat chromaffin cell. A, currents evoked with pulses from holding potential (H.P.) of -80 mV to test potentials (V_t) between -60 and $+60$ mV, only 4 traces are selected for presentation. Current traces were corrected for linear leak and capacitive current. B, averaged steady-state current (area under the solid bar in Fig. 1A) plotted against test potential for the traces shown in A. C, current trace evoked by long duration (2 sec) test potential to evaluate inactivation time constant (τ).

around +10 mV, and becomes smaller with progressively higher depolarizing pulses (Fig. 1B). Long depolarizing pulse (2 sec duration) was applied to determine the inactivation kinetics. Fig. 1C shows the typical current traces evoked by depolarization from -80 mV to 10 mV. If assuming this current is single exponential decaying current, the inactivation time constant (τ) was 1285 msec and its amplitude (A_1) was -121 pA and correlation coefficient was 0.991. If assuming double exponential decaying current, the longer time constant (τ_L) and amplitude (A_1) were 1510 msec and -126 pA. The shorter one (τ_S) and amplitude (A_2) were 39.1 msec and -16.4 pA. The correlation coefficient of double exponential fitting was 0.992.

Single exponential decay : $f(t) = A_0 + A_1 e^{-t/\tau}$

Double exponential decay :

$$f(t) = A_0 + A_1 e^{-t/\tau_L} + A_2 e^{-t/\tau_S}$$

During steady state current, the current was well fitted to single component of exponential, because amplitude (A_2) of τ_S and τ_S itself were very small in comparison with those of τ_L and correlation coefficients of single exponential fitting and double exponential fitting are almost same. So we used only τ as if the Ca^{2+} current were single exponential decaying current.

The effect of dihydropyridine (Fig. 2)

Nicardipine produced concentration-dependent block of Ca^{2+} currents of rat chromaffin cells. $1\mu\text{M}$ of nicardipine could block 71 % of peak current and 83 % of steady state current and $10\mu\text{M}$ of nicardipine could almost completely block the Ca^{2+} current (Fig. 2). Three cells were treated with $1\mu\text{M}$ of nicardipine and the blocking effect on steady state current was significantly larger than that on peak current. At the peak, $63.1 \pm 5.6\%$ of control current was blocked and at the steady state, $89.2 \pm 5.4\%$ of control current was blocked ($p < 0.05$) and the more potent effect on steady state current implicates the fact that there are two components in Ca^{2+} channels and the nicardipine insensitive component inactivates fast. In the figure, the Ca^{2+} currents were recorded

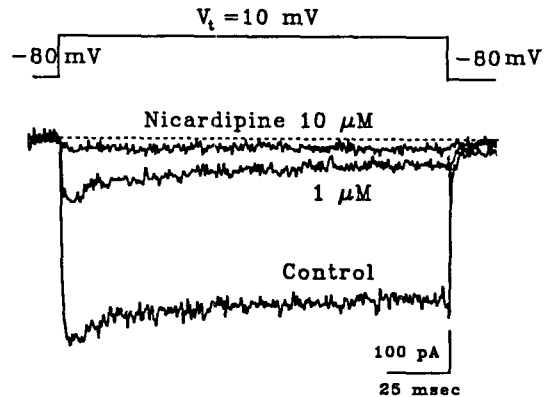


Fig. 2. Blockade of the long lasting Ca currents by nicardipine. The currents were activated by applying test potential of +10 mV from holding potential of -80 mV for 150 ms duration. Nicardipine ($10\mu\text{M}$): blockade of almost the current; nicardipine ($1\mu\text{M}$): blockade 71 % of peak current and 83 % of steady state current. The current traces were obtained from different cells but the cells were from the same culture dish (5th day of culture) and had the similar membrane capacitance (control: 5.35 pF ; $1\mu\text{M}$ pF : 4.62 pF ; $10\mu\text{M}$: 5.16 pF).

from different cells but the cells were of the same culture dish (5th culture day) and the similar membrane capacitance (control: 5.35 pF ; $1\mu\text{M}$: 4.62 pF ; $10\mu\text{M}$: 5.16 pF).

The effect of culture duration

We used the cells from the 1st culture day to the 7th culture day. The amplitude of current showed a trends of increase as the culture day passed by but the kinetic parameters like voltage dependence and inactivation time constant showed no difference along the culture duration. Fig. 3A presents the I-V relationships of each culture day. The current amplitudes were divided by the membrane capacitance (C_m) of each cell to normalize with the cell size and the normalized currents of each culture day were averaged to plot the I-V diagram. The voltage dependence of the current of each

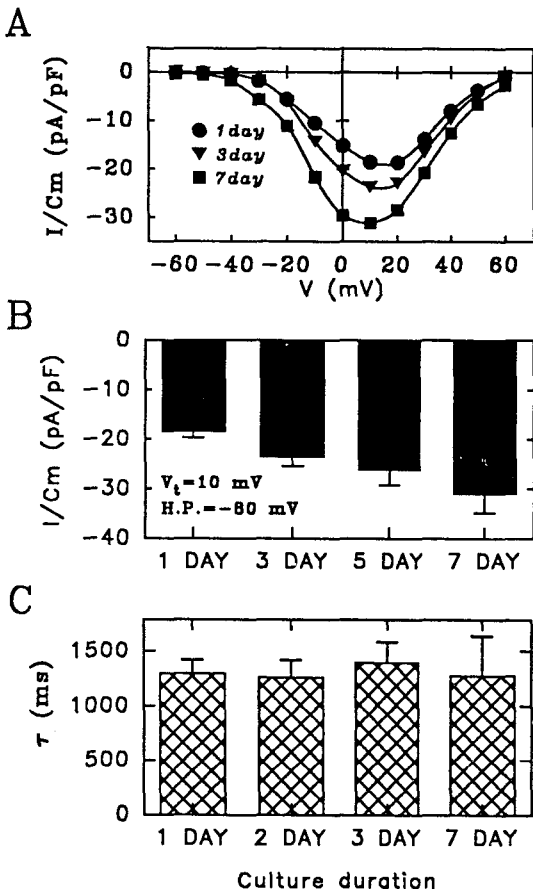


Fig. 3. Voltage dependence and τ 's of currents according to culture duration. A, the current-voltage relationships based on the culture duration. The normalized current amplitudes with membrane capacitance (I/C_m) were averaged to plot the mean values for diagram. B, Culture day and of normalized Ca^{2+} current. $V_t = +10$ mV, H.P. = -80 mV. C, Culture day and τ , fitted from the long-lasting (2 sec) trace. The values are not different according to culture duration.

culture day was not different. But the current amplitude was increased in along with the culture duration and statistically different (Fig. 3B, $p < 0.001$, ANOVA). Fig. 3C shows τ of the current of each culture day activated by 2 sec depolarization to 10 mV. There was no signifi-

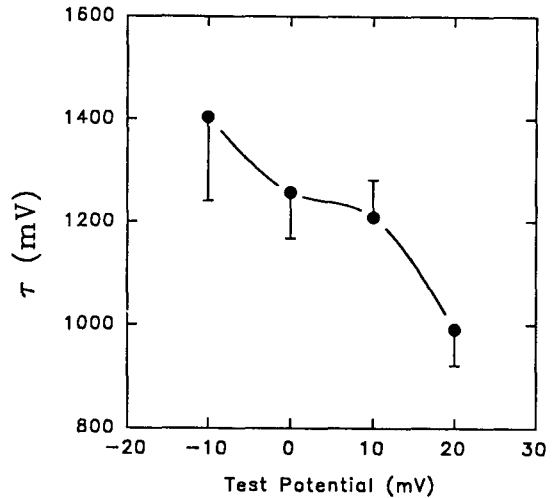


Fig. 4. Voltage dependence of time constants of Ca currents. The fitted values were obtained from the trace with long duration (2 sec) to various V_t from H.P. of -80 mV.

cant difference ($p > 0.05$). So we could pool the data of each culture day and evaluate the voltage dependence of τ . Fig. 4 show τ at each test potential. τ is decreased with progressive depolarization. This finding was similar to previous report (Fox et al., 1987). The mean, S.E.M., and size of observations are listed in Table 1.

The effect of various divalent cations

Divalent cations (Cd^{2+} , Co^{2+} , Ni^{2+} , Zn^{2+} and Mn^{2+}) were applied to evaluate the susceptibility of this long-lasting Ca^{2+} current. We applied various concentrations (in case of Cd^{2+} , Co^{2+} and Ni^{2+}) to delineate the dose-response curve. Mn^{2+} and Zn^{2+} were applied in fixed concentration ($100\mu M$) only to be compared with other cations for the affinity to Ca^{2+} channel.

The effect of Cd^{2+} . Various concentrations of Cd^{2+} were applied to the external solution to estimate the blocking effect of Cd^{2+} on Ca^{2+} currents. Fig. 5A presents the typical current traces that present the blocking effect of Cd^{2+} on Ca^{2+} currents. The current traces were obtained from different cells but the cells were of the same

Table 1. Voltage dependence of inactivation time constants

| V_t (mV) | τ | | | τ_L | | | τ_S | | |
|------------|--------|--------|------|----------|--------|------|----------|--------|------|
| | mean | S.E.M. | size | mean | S.E.M. | size | mean | S.E.M. | size |
| -10 | 1404.4 | 163.6 | 52 | 2215.2 | 308 | 34 | 46.1 | 11.1 | 34 |
| 0 | 1257.0 | 89.4 | 75 | 2123.9 | 235 | 43 | 60.1 | 9.4 | 43 |
| 10 | 1209.4 | 72.8 | 87 | 1825.3 | 146.1 | 63 | 60.9 | 5.4 | 63 |
| 20 | 991.4 | 70.8 | 80 | 1806.2 | 246.8 | 48 | 82.8 | 21.6 | 48 |

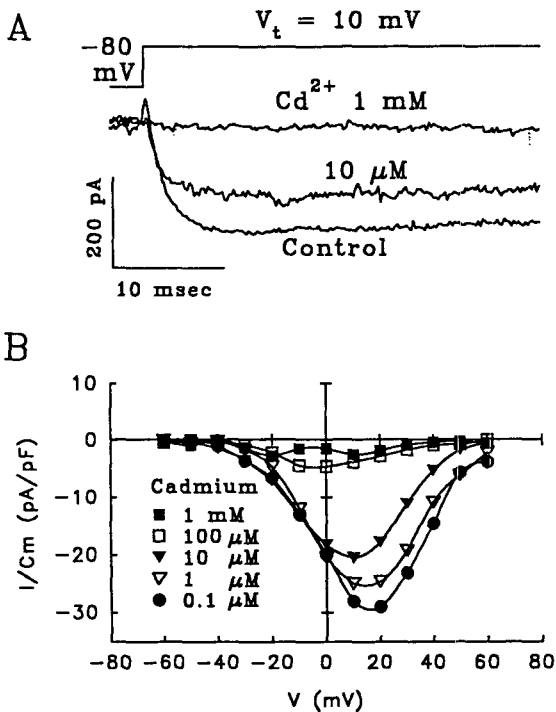


Fig. 5. Blockade of Ca current by Cd²⁺. A, current traces showing concentration dependent block of Ca²⁺ current. H.P. = -80 mV; V_t = +10 mV, 40 msec. The first trace current: obtained from the cell treated with 1 mM of Cd²⁺; the second trace: 10 μM of Cd²⁺; the last trace: control condition. B, the average of normalized steady state current plotted against test potential. The each conditions are described in table 2.

culture dish and had the similar membrane capacitance. The blocking effect of Cd²⁺ on Ca²⁺

current was increased according to the increase of concentration of Cd²⁺ in bath solution. Cd²⁺ 1 mM could block completely the Ca²⁺ current. The current amplitudes were divided by the membrane capacitance of each cell to normalize with the cell size. The normalized currents of each concentration of Cd²⁺ were averaged to plot the I-V diagram (Fig. 5B). The voltage dependence of the current of each concentration of Cd²⁺ was not different and the right shift tendency of peak amplitude in I-V diagram did not have any statistical meaning. The I-V relationship of control current was identical to I-V relationship in the presence of 0.1 μM Cd²⁺, so the control was not shown. The mean and S.E.M. of amplitude ratio of the current of each concentration of Cd²⁺ to the control current was listed in Table 2. All current amplitudes were obtained by depolarization to +10 mV.

The effect of Co²⁺. Various concentrations of Co²⁺ were applied to the external solution to estimate the blocking effect of Co²⁺ on Ca²⁺ currents. Fig. 6A presents the typical current traces that present the blocking effect of Co²⁺ on Ca²⁺ currents. The current traces were obtained from different cells but the cells were of same culture dish and had the similar membrane capacitance. The blocking effect of Co²⁺ on Ca²⁺ current was increased according to the increase of concentration of Co²⁺ in bath solution. Co²⁺ 10 mM could block completely the Ca²⁺ current. As the case of Cd²⁺, I-V diagrams of Co²⁺ were obtained (Fig. 6B). The voltage dependence of the Ca²⁺ current of each concentration of Co²⁺ is not different. As the case of Cd²⁺, the I-V relationship of control current was also identical to I-V rela-

Table 2. Means of calcium current ratio in the presence of cations. Mean, S.E.M., size at different concentration (Conc.) are presented

| Conc. | Cadmium | | | Cobalt | | | Nickel | | |
|-------------------|---------|--------|------|--------|--------|------|--------|--------|------|
| | Mean | S.E.M. | Size | Mean | S.E.M. | Size | Mean | S.E.M. | Size |
| 0.1 μM | 0.9552 | 0.0810 | 7 | 0.8262 | 0.0670 | 5 | 0.9177 | 0.1590 | 7 |
| 1 μM | 0.9611 | 0.0829 | 7 | 0.8823 | 0.0934 | 9 | 0.8263 | 0.1007 | 12 |
| 10 μM | 0.9035 | 0.1360 | 7 | 0.9096 | 0.1005 | 9 | 0.7492 | 0.0873 | 3 |
| 100 μM | 0.2097 | 0.0329 | 6 | 0.4650 | 0.1726 | 3 | 0.7809 | 0.1309 | 3 |
| 1 mM | 0.0237 | 0.0161 | 5 | 0.2159 | 0.0516 | 4 | 0.5210 | 0.2128 | 3 |
| 10 mM | | | | 0.0390 | 0.0198 | 4 | 0.0000 | 0.0000 | 6 |

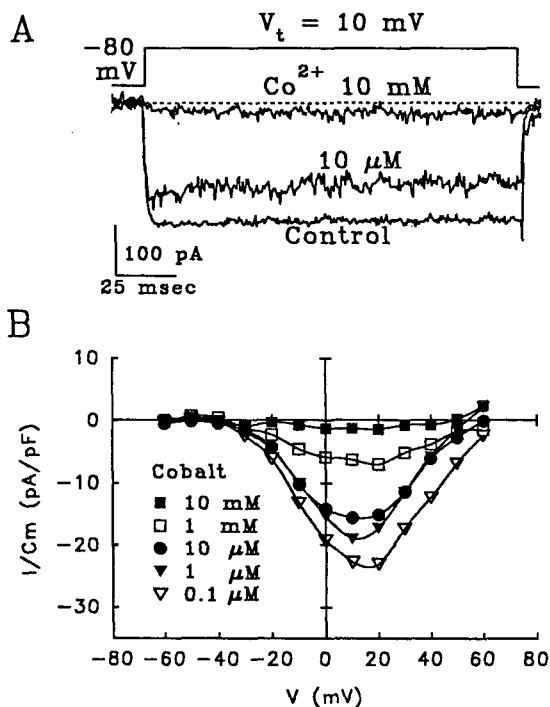


Fig. 6. Blockade of Ca current by Co²⁺. A, current traces showing concentration dependent block of voltage dependent Ca²⁺ current. H.P. = -80 mV; V_t = +10 mV, 150 msec. The first current trace obtained from the cell treated with 10 mM of Co²⁺; the second trace: 10 μM of Co²⁺; the last trace: control condition. B, the average of normalized steady state current plotted against test potential. The size of each condition are described in table 2.

relationship in the presence of 0.1 μM Co²⁺. The mean and S.E.M. of amplitude ratio of the current of each concentration of Co²⁺ to the control current was listed in Table 2. All current amplitudes were obtained with V_t to +10 mV.

The effect of Ni²⁺. Various concentrations of Ni²⁺ were applied to the external solution to estimate the blocking effect of Ni²⁺ on Ca²⁺ currents. Fig. 7A presents the typical current traces. The current traces were obtained from different cells but the cells were of same culture dish and had the similar membrane capacitance. The blocking effect of Ni²⁺ on Ca²⁺ current was increased according to the increase of concentration of Ni²⁺ in bath solution but its effect was the lowest. 1 mM Ni²⁺ could block only 48.9 % of control Ca²⁺ current. As the case of Cd²⁺, I-V diagrams of Ni²⁺ were obtained (Fig. 7B). The voltage dependence of the Ca²⁺ current of each concentration of Ni²⁺ is not different. The I-V relationship of control current was also identical to I-V relationship in the presence of 0.1 μM Ni²⁺, so the control was not shown. The mean and S.E.M. of amplitude ratio of the current of each concentration of Ni²⁺ to the control current was listed in Table 2. All the current amplitude was obtained by depolarization to +10 mV.

Dose-response curves. Fig. 8 shows the dose response curve of each divalent cation. Amplitude ratio of the current of each concentration of divalent ions to the control current was calculated after the normalization of steady

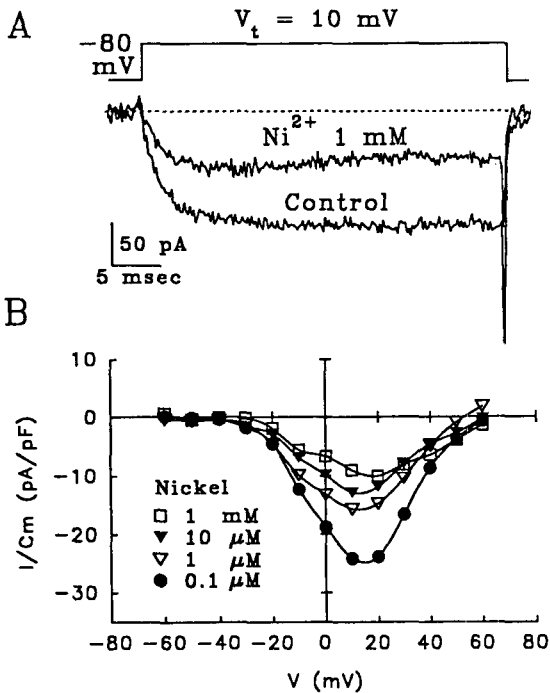


Fig. 7. Blockade of Ca current by Ni²⁺. *A*, current traces showing concentration dependent blockade of Ca²⁺ current activated by 40 msec depolarizations. Note the tail current with short duration of depolarization. H.P. = -80 mV, V_t = +10 mV. The first trace current obtained from the cell treated with 1 mM of Ni²⁺; the second trace: control condition. *B*, the averaged value of normalized steady state current plotted against test potential. To see the size of each condition, refer to table 2.

state current amplitude with C_m. And its value was fitted on the semilogarithmic scale. Assuming 1:1 dose-response relationship, the equilibrium dissociation constant (K_d) of Cd²⁺ was 39 μM, K_d of Co²⁺ was 100 μM, and K_d of Ni²⁺ was 780 μM. The means of each divalent cations at the same concentration (100 μM) were compared and were significantly different (p < 0.05) by the ANOVA with single factor. At the concentration of 100 μM, Zn²⁺ blocked 36.2 ± 11.7 % of Ca²⁺ currents (n = 5), Mn²⁺ blocked 39.5 ± 19.1 % of Ca²⁺ currents (n = 4). So they also had blocking effects on Ca²⁺

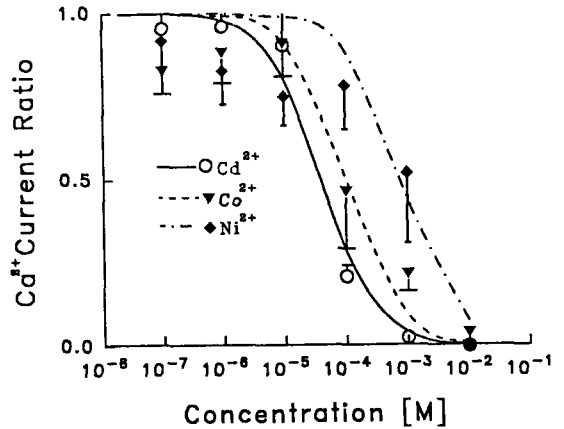


Fig. 8. Dose-response curves. Averaged steady-state Ca current ratio to the control currents in the presence of increasing concentrations of divalent cations was plotted. Ca²⁺ current ratio is the ratio between the averaged normalized current in the presence of divalent cations to the averaged control current. The data in the presence of Cd²⁺ were fitted by a 1:1 dose-response curve with equilibrium dissociation constant (K_d) of 39 μM at the H.P. of -80 mV to V_t of +10 mV. K_d of Co²⁺ was 100 μM and K_d of Ni²⁺ was 780 μM. The mean, S.E.M. and size of each condition are described in table 2.

current.

DISCUSSION

The principle findings of this study are as follows. First, the majority of Ca²⁺ channels in rat chromaffin cells are well classified to L-type Ca²⁺ channel from the data of kinetics and pharmacology. This Ca²⁺ current of our rat chromaffin cells has long τ above 1000 ms and begins to be activated about -40 mV and is highly sensitive to dihydropyridine. So we refer this Ca²⁺ channel to L-type. Second, the blocking effect of Cd²⁺ is the most potent among the treated cations; Co²⁺, Ni²⁺, Zn²⁺ and Mn²⁺ also have blocking effects on Ca²⁺ current.

Ca²⁺ currents in our cell were activated at V_t

over -40 mV and inactivated with very slow time course. Comparing with the original reports of L- and N-type Ca^{2+} channel (Nowycky et al, 1985; Fox et al., 1987), the kinetic characteristics of our cell was identical to those except the point that the current was activated at somewhat lower potential. Fox et al. (1987) reported L-type currents in chick sensory neuron activated at V_i of -10 mV but Ca^{2+} current isolated from the bovine chromaffin cell showed very similar voltage dependence to our result (Fenwick et al., 1982). Although conclusions of many previous studies relied on these kinetic distinctions of Ca^{2+} channels, we could not easily conclude that the channel type of Ca^{2+} channels in our cell was L-type with kinetic analysis only. Recent report denied the fact that inactivation kinetics and sensitivity to holding potential can resolve these two channels (Cox and Dunlap, 1992). Therefore the pharmacological evidence was essential for channel typing and the high affinity of our cell to dihydropyridines supported that our cell has the L-type Ca^{2+} currents. Furthermore we measure the currents at the plateau phase to exclude the fast decaying other types of currents if exist, so we were sure to examine the effect of divalent cations on L-type Ca^{2+} channels.

The blocking effect of Cd^{2+} on L-type Ca^{2+} channels was more potent than that of Ni^{2+} . This fact is also consistent with the reported characteristics of L-type Ca^{2+} channel of neuronal cell (Fox et al., 1987; Tsien et al., 1988). Ni^{2+} was the least potent blocker of which we had tried. We could not see the complete block even at the concentration of 10 mM of Ni^{2+} . The potent blockade of Ca^{2+} currents with Cd^{2+} is inconsistent with the fact that the amount of catecholamines release from the adrenal gland perfused with 100 μM of Cd^{2+} , Ni^{2+} did not decreased in the rat (Shukla & Wakade, 1991). At the concentration of 100 μM Cd^{2+} , the Ca^{2+} current was reduced to $20.9 \pm 3.2\%$ of control value. This discrepancy suggests the possibility that secretory process can be operated without the influx of Ca^{2+} through Cd^{2+} sensitive L-type Ca^{2+} channels in the rat adrenal glands if both results were not

mutually contradictory. The Ca^{2+} influx through Cd^{2+} insensitive channels could be the Ca^{2+} source for the secretory process.

Although the majority of Ca^{2+} channels in rat chromaffin cells were classified to L-type Ca^{2+} channel, we could not excluded the existence of other types of Ca^{2+} channels and the variety of τ supports the variable distribution of minor different Ca^{2+} channels. The mean values of τ were longer than 1 sec but the distribution of τ was diverse: a part (10 of 81 cells) of Ca^{2+} current inactivated with τ under 500 msec or so. Fenwick et al. (1982) already pointed out that current traces differed from cell to cell on a kinetic basis and this fact revealed that each curve might be the sum, in variable portion, of L- and other minor contributing component (Bossu et al., 1991). In the case of the cell demonstrated in Fig. 1, the proportion of minor component could be calculated, based on the fitted amplitudes of double exponential fitting, to 11% of total peak current. Existence of subpopulations of cells was reported in other neuronal organ (Cox & Dunlop, 1992; McCarthy & TanPiengco, 1992) and Cox and Dunlop (1992) suggested that the expression N- and L-type Ca^{2+} channels are dependent on duration of culture. The correlation of τ with culture duration was not observed in our results (1 to 7 day of culture) and the correlation with other factor could not be found through our data. The characteristics and physiological meaning of that minor component of Ca^{2+} current in rat chromaffin cell are the subjects of further exploration.

REFERENCES

- Akaike A, Mine Y, Sasa M & Takaori S (1990) Voltage and current clamp studies of muscarinic and nicotinic excitation of the rat adrenal chromaffin cells. *J Pharmacol Exp Ther* **255**, 333-339
- Artalejo C, Ariano M, Perlman RL & Fox AP (1990) Activation of facilitation calcium channels in chromaffin cells by D1 dopamine receptors through a cAMP/protein kinase A-

- dependent mechanism. *Nature* **348**, 239-241
- Artalejo C, Dahmer MK, Perlman RL & Fox AP (1991a) Two types of Ca²⁺ currents are found in bovine chromaffin cells: Facilitation is due to the recruitment of one type. *J Physiol* **432**, 681-707
- Artalejo C, Perlman RL & Fox AP (1991b) ω -conotoxin inhibits a Ca²⁺ current in bovine chromaffin cells that does not seem to be N-type. *Biophys J* **59**, 369a (Abstract)
- Augustine GJ & Neher E (1992) Calcium requirements for secretion in bovine chromaffin cells. *J Physiol* **450**, 247-271
- Ballesta JJ, Palmero M, Hidalgo MJ, Gutierrez LM, Reig JA, Viniegra S & Garcia AG (1989) Separate binding and functional sites for ω -conotoxin and nitrendipine suggest two types of calcium channels in bovine chromaffin cells. *J Neurochem* **53**, 1050-1056
- Cena V, Stutzin A & Rojas E (1989) Effects of calcium and Bay K-8644 on calcium current in adrenal medullary chromaffin cells. *J Memb Biol* **112**, 255-265
- Cox DH & Dunlap K (1992) Pharmacological discrimination of N-type from L-type calcium current and its selective modulation by transmitters. *J Neurosci* **12**(3), 906-914
- Douglas WW (1968) Stimulus-secretion coupling: the concepts and clues from chromaffin and other cells. *Brit J Pharmacol* **34**, 451-474
- Douglas WW. Secretomotor control of adrenomedullary secretion: synaptic membrane and ionic events in stimulus-secretion coupling. In: *Handbook of Physiology*, Sect 7, Vol 6 (Blashko H, Sayers G and Smith AD eds.), pp 366-388, Washington DC, 1975
- Fenwick EM, Marty A & Neher E (1982) Sodium and calcium channels in bovine chromaffin cells. *J Physiol* **331**, 590-635
- Fox AP, Nowycky MC & Tsien RW (1987) Kinetic and pharmacological properties distinguishing three types of calcium currents in chick sensory neurons. *J Physiol* **394**, 149-172
- Hamill OP, Marty A, Neher E, Sakmann B & Sigworth FJ (1981) Improved patch clamp techniques for high-resolution current recording from cells and cell-free membrane patches. *Pflugers Arch* **391**, 85-100
- Kim YI & Neher E (1988) IgG from patients with Lambert-Eaton syndrome blocks voltage-dependent calcium channels. *Science* **239**, 405-408
- Lambert EH & Elmquist E (1971) Quantal components of end-plate potentials in the myasthenic syndrome. *Ann NY Acad Sci* **183**, 183-191
- Lang B, Newsom-Davis J, Peers C, et al. (1987) The effects of myasthenic syndrome antibody on presynaptic calcium channels in the mouse. *J Physiol* **390**, 257-270
- McCarthy RT & TanPiengco PE (1992) Multiple types of high-threshold calcium channels in rabbit sensory neurons: High-affinity block of neuronal L-type by nimodipine. *J Neurosci* **12**(5), 2225-2234
- Neher E & Marty A (1982) Discrete changes of cell membrane capacitance observed under conditions of enhanced secretion in bovine adrenal chromaffin cells. *Proc Natl Acad Sci USA* **79**, 6712-6716
- Nowycky M, Fox AP & Tsien RW (1985) Three types of neuronal calcium channel with different calcium agonist sensitivity. *Nature* **316**, 440-443
- Rosario LM, Soria B, Feuerstein G & Pollard HB (1989) Voltage-sensitive calcium flux into bovine chromaffin cells occurs through dihydropyridine-sensitive and dihydropyridine- and ω -conotoxin-insensitive pathways. *Neurosci* **29**, 735-747
- Shukla R & Wakade AR (1991) Functional aspects of calcium channels of splanchnic neurons and chromaffin cells of the rat adrenal medulla. *J Neurochem* **56**, 753-758
- Tsien RW, Madison DV, Lipscombe D & Fox AP (1988) Multiple types of Neuronal calcium channels and their selective modulation. *Trends in Neurosci* **11**, 431-437
- Wakade AR, Malhotra RK & Wakade TD (1986) Phorbol ester facilitates 45Ca accumulation and catecholamine secretion by nicotine and excess K⁺ but not by muscarine in rat adrenal medulla. *Nature* **321**, 698-700